Available online at www.jourcc.com

Journal homepage: www.JOURCC.com

Journal of Composites and Compounds

Effect of the powder manufacturing process on characteristics of nanostructured MCrAlY coatings: dry vs. wet ball milling

Ali Zakeri [a], Pouya Tahvili [a], Elnaz Bahmani [a], Alireza Sabour Rouh Aghdam [a]*

[a] *Department of Materials Engineering, Tarbiat Modares University, Tehran P.O. Box: 14115-143, Tehran, Iran*

A B S T R A C T

Metallic MCrAlY coatings have been widely utilized to protect the high-temperature materials operating in aggressive conditions of gas turbines. However, with more demands on the turbine inlet temperature rise for efficiency gains, there is a need to further improve the high-temperature performance of the MCrAlY coatings. A possible way to meet this challenge is by microstructure modification. The aim of this study is to produce nanocrystalline MCrAlY powders via wet and dry mechanical milling techniques and deposit the obtained feedstock powders by the high-velocity oxygen fuel (HVOF) spraying method. Comprehensive characterization and comparison of the different powder processing techniques and the corresponding coatings were studied. It was established that the nano-scaled MCrAlY feedstock powder with low contamination levels could be achieved by mechanical milling. Moreover, the powder samples were well-deposited by the HVOF process and the correlation between powder properties and coating characteristics was investigated.

Peer review under responsibility of JCC Research Group

A R T I C L E I N F O R M A T I O N

Article history:
Received 07 January 2021
Received in revised form 11 February 2021
Accepted 27 March 2021

Keywords:
MCrAlY
Ball milling
Thermal spray
HVOF

1. Introduction

In today's modern world, it is well-known that the gas turbines have dominated the electricity generation and aerospace industries [1]. The incentive and driving force for further developing the advanced gas turbines arise from the society's increasing demand for aviation and electricity industries [2]. This could be achieved through increasing the inlet temperature of these engines, which translates to their higher efficiency. In addition, the higher efficiency plays a key role in the carbon emission reduction due to lower fossil fuel consumption. That being said, higher operating temperatures lead to more aggressive conditions for engine components; therefore, new materials with enhanced thermo-mechanical properties along with more efficient protective coatings are vital for successful prolonged operation of the engines [3–6].

It has been reported that up to 50% of the total weight of a gas turbine powered aircraft is manufactured from Ni-based superalloys [7]. However, it should be taken into account that the primary role of these alloys is to endure the heavy mechanical loads at the elevated temperatures; therefore, the design strategy is to maximize the mechanical strength at the expense of environmental degradation resistance [8]. In this respect, the protective coatings came into being. The most commonly used coatings for the protection of superalloy components consist of chromia- and alumina-forming alloys. Oftentimes, these coatings are applied via diffusion treatments and thermal spraying methods, which have gained popularity in the industry [9–12]. MCrAlY-type alloys (M: Ni and/or Co) are considered the state-of-the-art materials for thermal spray coatings and have proven to be effective in most engine applications [13]. Furthermore, it has been shown that MCrAlY coatings can be deposited by HVOF process, which enjoy equivalent, and sometimes superior, protection properties compared to the plasma-sprayed counterparts [14–16].

Although utilizing the conventional coatings have enabled the superalloy components to serve at harsh conditions, further advancements in gas turbine efficiency are conditional to the development of thermostable and oxidation-resistant coatings [17]. One of the practical approaches for this purpose is the microstructural modification of coatings. In this regard, some routes have been proposed and pursued by other researchers, some good examples of which are: powder processing, laser treatment, and shot peening [18–21]. Among these approaches, the powder processing via mechanical milling technique has been widely adapted due its simplicity and versatility [14, 22].

The mechanical milling is a solid-state powder processing technique which is applicable to a number of purposes, including grain refinement, inducing preferred orientation, and homogeneous dispersion of reinforcements in a multicomponent powder system [22]. In a study by Tahari et al., CoNiCrAlY/YSZ composite powders with nanocrystalline structure and uniform dispersion of strengthening ceramic particles were produced via mechanical milling process [23]. Studies conducted by Ajdelsztajn et al. have confirmed the capability of HVOF process to produce the nanostructured MCrAlY coatings by virtue of its high kinetic energy and low spraying temperature [24–26]. Despite research efforts highlighting the characteristics of nanostructured MCrAlY powders and coatings, it is essential to examine the effects of mechanical milling conditions and their influence on the quality of final coatings in terms of the desired microstructure and oxidation performance. Given this

* *Corresponding author: Ali Zakeri; E-mail: alizakeri@modares.ac.ir*
DOR: 20.1001.1.26765837.2021.3.6.2.5
https://doi.org/10.52547/jcc.3.1.2

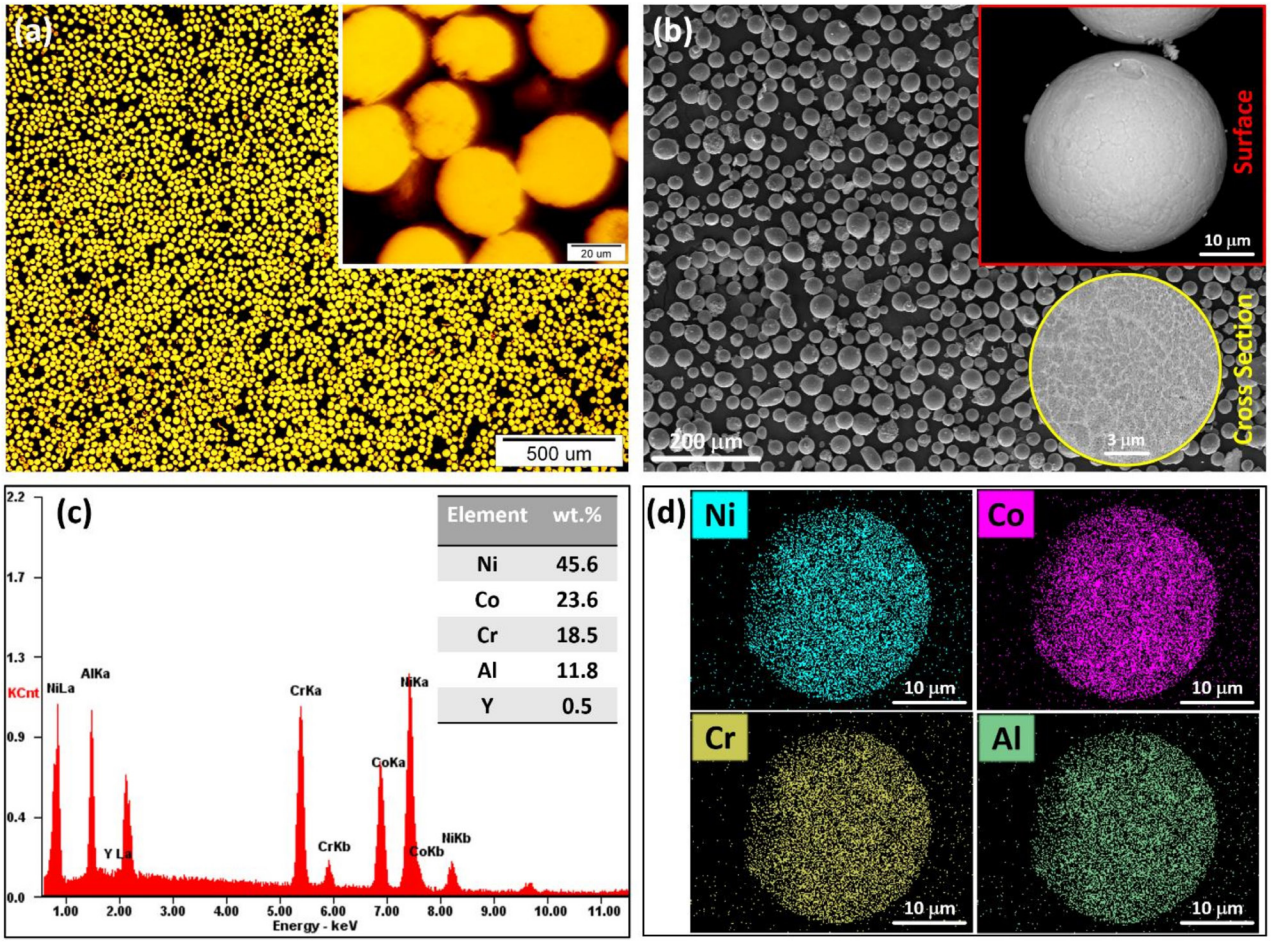

Fig. 1. Morphology and chemical composition of the as-received NiCoCrAlY powder; (a) optical light micrographs of powder cross-section, (b) SEM images (the inset images show the secondary electron (SE) and backscattered electron (BSE) mode images from the surface and cross-section, respectively), (c) EDS analysis, and (d) EDS elemental mapping.

background, the objective of current work concerns with the feedstock powder characteristics-microstructural evolution relationship of the nanostructured MCrAlY coatings produced by the mechanical milling.

2. Material and methods

2.1. Powder materials and processing

A commercially available gas-atomized MCrAlY powder supplied by Oerlikon Metco was used as the starting powder material (Fig. 1). The preparation of the nanostructured feedstock powder was carried out by using a two-body planetary ball milling machine. Prior to the milling, the vials were purged with argon gas to prevent possible powder oxidation. Two modes of milling, namely dry and wet milling, were conducted. The sample coding along with the milling conditions of each powder are given in Table 1. As is known from the selected milling parameters, the only difference is the amount of process control agent, also known as surfactant or lubricant, used for each mode. Typically, PCAs are organic compounds commonly used in the milling processes. Basically, these compounds are surface-active agents which can be adsorbed on the powder particles' surfaces, by which they control the milling mechanism [22]. As will be discussed in the next section, the WM powder was followed by an additional spray drying process to provide the suitable morphology of the powder for thermal spraying. This process was performed using a high-speed centrifugal spray drier with the inlet and outlet temperature values of 350 and 120 ℃, respectively. The rotating speed of the atomizing disc was set to 10500 rev/min. It worth noting that no binder was added to the powder slurry before feeding into the spray dryer and the final product was used as the feedstock powder without any post calcination treatments.

Table 1.
Sample coding and milling conditions for the powder specimens.

Sample (Code) / Parameter	Revolution Speed (RPM)	Ball to Powder Ratio (wt.%)	Process Control Agent (PCA)	Milling Time (h)
Conventional (CN)	-	-	-	-
Dry Milled (DM)	200	20:1	Ethanol (1 wt.%)	10
Wet Milled (WM)	200	20:1	Ethanol (5 wt.%)	10

2.2. HVOF thermal spraying

A commercial HVOF system was used for the deposition of MCrAlY coatings. Ground and degreased mild steel coupons (60 × 30 × 2 mm^3) were used as the substrate. Owing to the fact that in this study, the coatings were characterized in the free-standing form, no traditional preparation of the substrate, such as grit blasting, was conducted prior to the thermal spraying. The spraying parameters, for all three types of the powders, were chosen based on the conventional powder manufacturer's recommendation. With this respect, the thermal spraying was carried out with an oxygen flow rate of 200 l/min, propane flow rate of 55 l/min, and at a spraying distance of about 28 cm. It is worth noting that the maximum flame temperature of 2828 ℃ can be reached using the

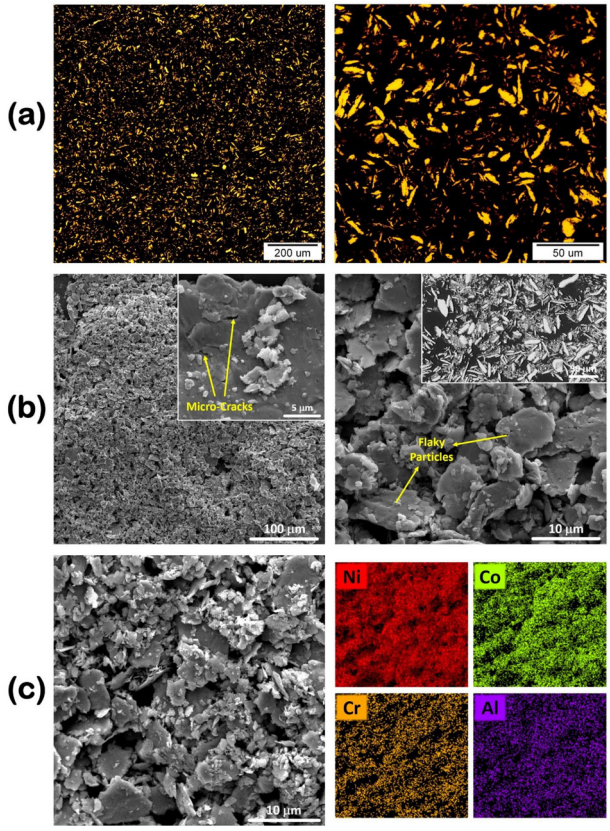

Fig. 2. As-milled WM powder; (a) OM images, (b) secondary electron SEM images (the inset image in the right presents the BSE-SEM image from the cross-section), and (c) SEM images with the corresponding EDS elemental mapping.

propane-oxygen mixture with the oxygen to propane ratio of 4.5 [27].

2.3. Characterization techniques

The microstructure of the obtained powders and coatings were observed by optical light microscopy (OM, Olympus BX51, Olympus Optical Co., Ltd., Japan). The surface morphology and cross-section examinations were performed by scanning electron microscopy (SEM, Ziess EVO MA15) equipped with an EDS detector (EDAX Genesis and Oxford Instruments). In addition, the high-magnification images were taken with a field-emission scanning electron microscope (FESEM, Nova NanoSEM 450). According to the ASTM E-384 standard, a microhardness tester instrument (MicroMet 1, Buehler) was used for the hardness measurements, using a load of 300 g [28]. The reported values are based on the average of at least ten measurements.

3. Results and discussion

3.1. Powder characterization

Fig. 2 shows the OM and SEM-EDS analyses of as-milled WM powder. Compared to the original spherical morphology, severe particle deformation can be clearly observed with the morphological transformation to the flaky particles. Despite the fact that the NiCoCrAlY powder is consisted of a ductile g-matrix with FCC crystal structure, the typical tendency for cold-welding was inhibited, primarily due to the active presence of ethanol [14]. Also, some micro-cracks were observed on the surface of particles (Fig. 2b) which indicates the fracturing stage as the dominant mechanism controlling the milling process. A combined effect of the ethanol inhibiting the cold welding and the work-hardening of particles through the milling process led to the dominance of fracturing stage. According to the EDS mapping analysis (Fig 2c), the milling process did not affect the chemical composition homogeneity. Further, it has been confirmed that high-energy ball milling could induce nanocrystallization in the milled powder samples [22]. This is true in the case of as-milled WM powder and the nano-scale structure of the powder particles were confirmed through high-magnification FESEM images (Fig. 3). As is well-known, the nanocrystalline materials have significantly higher diffusion rates in comparison to the materials with conventional grains size; typically, greater than 1 mm. This specific property favors the oxidation performance of MCrAlY coatings owing to the fact that the protective oxide former element (Al) benefits the higher diffusion flux to the coatings surface and developing a protective alumina scale in less time [29 31].

Analyzing the microscopic morphologies shows that the as-milled WM powder particles do not satisfy the suitable powder properties for the HVOF spraying process, namely the spherical morphology with a size distribution of 10–45 mm [32]. This is because the small-sized particles have small mass inertias and they might not track the motion of HVOF jet stream, which in turn reduces the deposition efficiency [33]. With this in mind, a subsequent spray drying process was utilized to obtain powder particles which meet the requirements of HVOF feeding system. Fig. 4 depicts the OM and SEM images of the spray-dried WM powder. It can be seen that the obtained granules are composed of semi-spherical shaped particles with diameters in the range of 10-50 mm. With respect to these characteristics, it is reasonable to predict that the spray-dried powder particles benefit from good flowability in the HVOF jet stream. Moreover, it is evident that each particle contains building blocks of flaky-shaped fractures shown in Fig. 2b. Based on the cross-section and surface morphology of the particles, it is clear that the granules are not completely dense and compact. Since the particle formation during the spray drying process involves the agglomeration of small particles, some hollow or porous particles might be observed in the final product [34].

Fig. 5 displays the OM and SEM images of the DM powder. As can be observed, the milling process in the dry condition has resulted in the semi-spherical powder particles. As opposed to the spray-dried sample, DM powder particles are compact and intensely cold-welded. It should be taken into account that the amount of PCA used for the milling of DM powder was lower than that of WM powder; therefore, the milling medium was dry for most of the milling time. Considering this, it appears that the absence of ethanol has promoted the cold-welding mechanism, producing the semi-spherical agglomerates which did not require any granulation process for using as the HVOF feedstock powder.

Despite the advantages of the mechanical milling, powder contamination has been remained as one of the main limitations of this process. Owing to the nanostructure characteristics of milled powder particles, namely large surface area and small size of the particles, some precautions should be taken to minimize the introduction of impurities. That being said, it can be surmounted by optimizing the milling parameters and using the proper materials as the PCA and grinding medium. The different results reported by the researchers, showing different levels of impurities, indicate the significant role of the milling conditions, including atmosphere, intensity and time of milling. The inherent properties of the powder samples, such as strength and hardness, influence the powder contamination as well [13]. Fig. 6 reports the EDS analysis results from the final powder samples in this study. It is apparent that the level of Fe impurity is higher in the case of dry milling condition. This can be attributed to the wear of the grinding balls and vials, which occur at a higher rate in the dry milling conditions. It should be noted that the impurity levels detected in this study are relatively low; hence, it would neither affect the microstructure nor the oxidation properties of the MCrAlY coatings [16, 35].

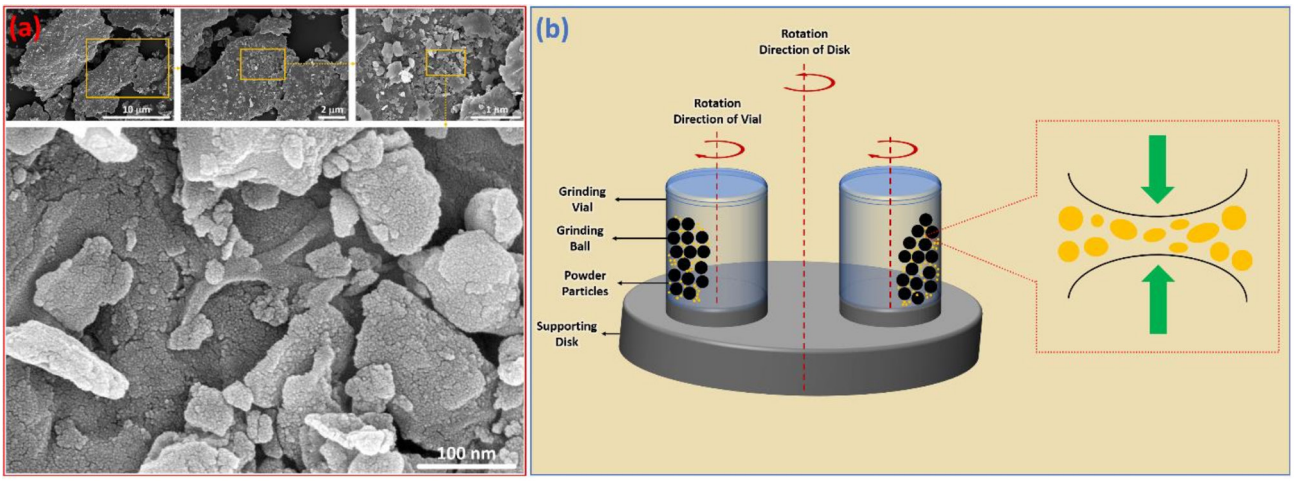

Fig. 3. (a) High-magnification FESEM images of the as-milled WM powder and (b) a schematic representing the mechanical milling process.

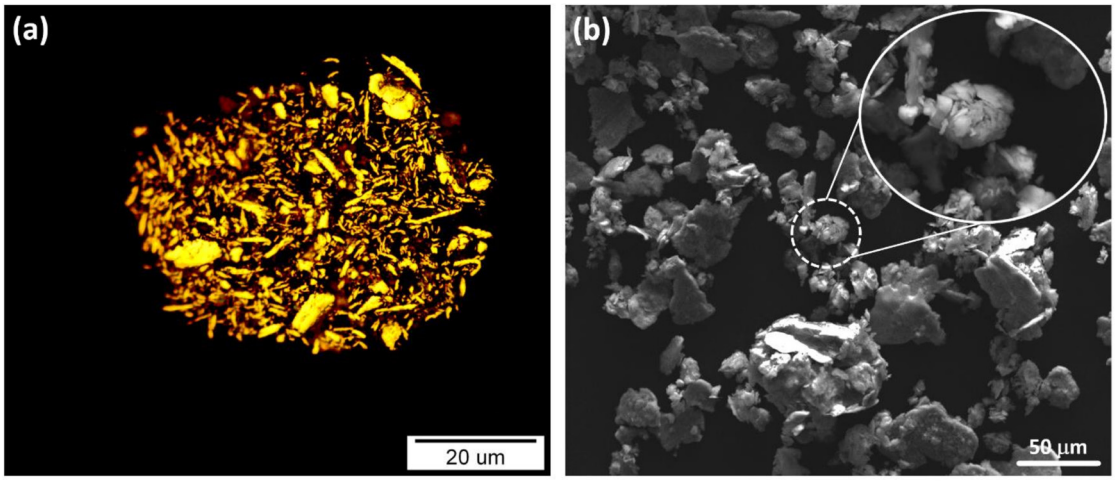

Fig. 4. Spray-dried WM powder; (a) cross-sectional OM image and (b) secondary electron SEM image.

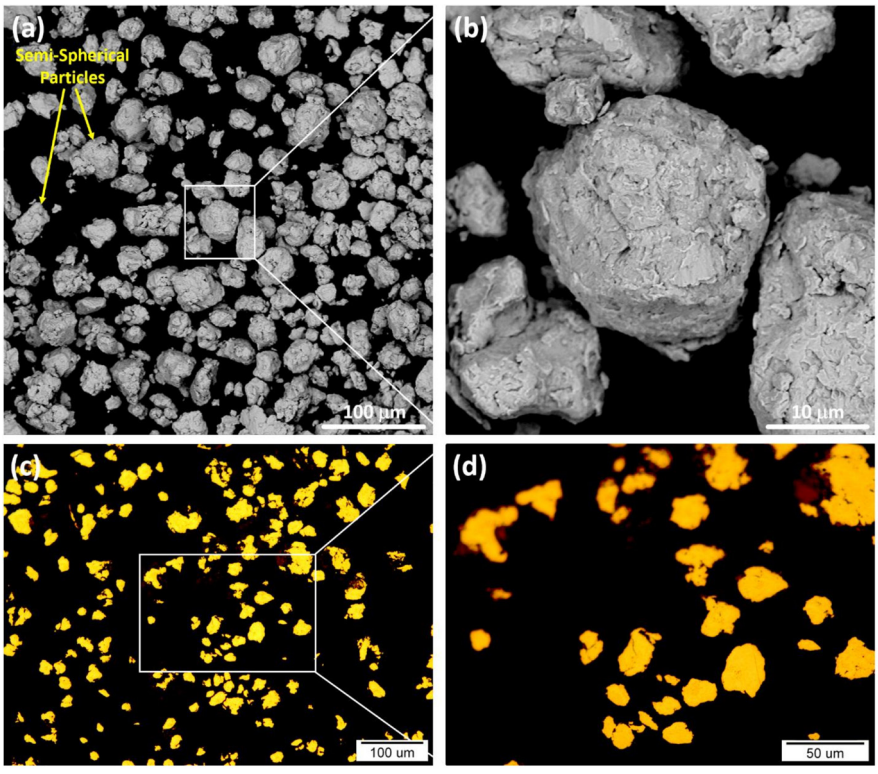

Fig. 5. DM powder; (a, b) secondary electron SEM images and (c, d) cross-sectional OM images.

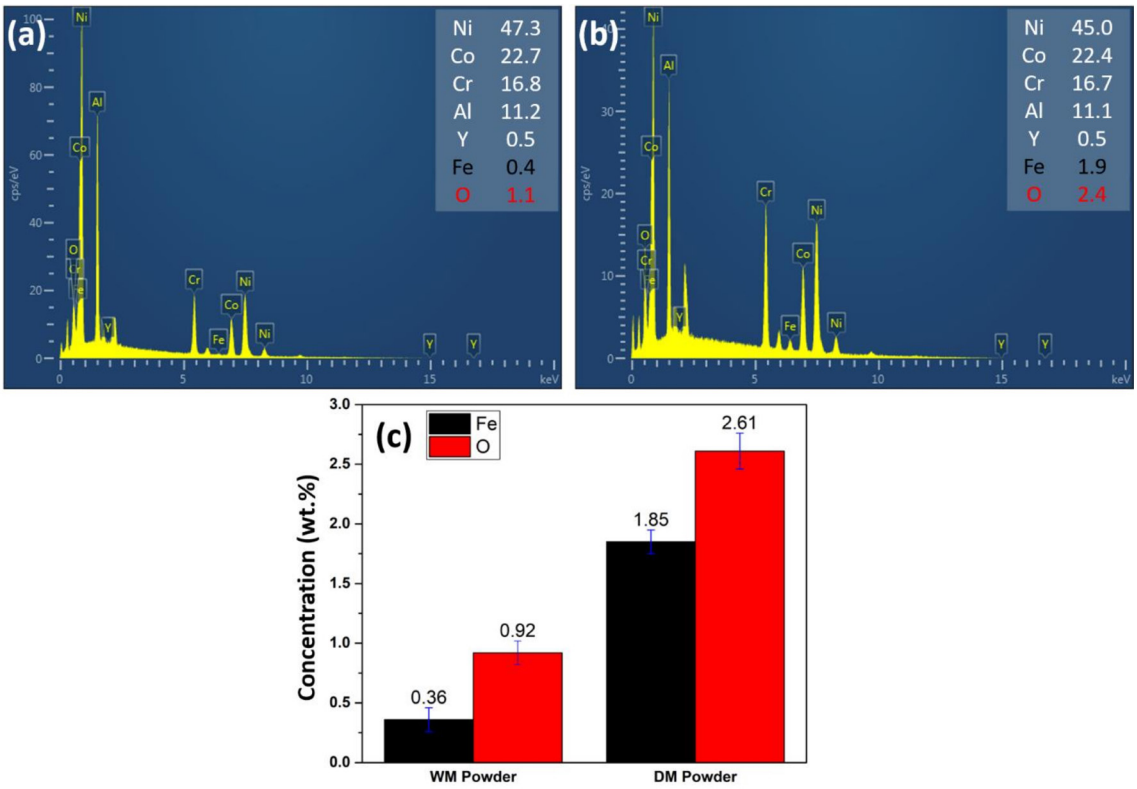

Fig. 6. EDS analysis results from (a) WM and (b) DM powders with a comparison of mean values of O and Fe contents shown in (c).

3.2. Coating characterization

The conventional NiCoCrAlY powder as well as the milled powders were sprayed by HVOF technique. Fig. 7 presents the characteristics of the CN coating. To better explain the coating characteristics, the HVOF deposition mechanism is briefly reviewed. In HVOF process, the desired feedstock material is injected into a high-velocity jet stream and heated up to get fully and/or partially melted. This is accompanied by the acceleration of the powder particles, followed by propelling onto the substrate and impinging in a semi-solid state. Upon the impact, the bonding of coating material takes place by mechanical interlocking. After the solidification of the impacted particles, they form splats in a lamellar manner [36].

Based on the Fig. 7a, it can be seen that a number of un-melted particles have maintained their original spherical morphology. This is mostly true for the larger particles which do not get as easily melted as the smaller ones. It is worth noting that the surface particles lack the impact pressure from the subsequent deposition pass; therefore, there is a higher possibility for the particles to experience a minor degree of deformation [14]. Moreover, splashed regions were also observed on the coating surface, as a result of molten particle impingement. The EDS point analysis from these areas showed a higher content of oxygen, which is probably due to the oxygen pick-up during the atmospheric spraying [37].

The cross-sectional investigations were performed in both SE and BSE modes of SEM. The SE-SEM image confirms the highly compact structure of the deposited coating, without any large pores. It should be mentioned that the pores are associated with some depth in the SE mode SEM images [38]. Some dark veins can be observed in the BSE-SEM image, indicating the splat boundaries. These dark lines were formed as a consequence of slight in-flight oxidation and are mainly composed of Al oxide. Moreover, the gray-colored b precipitates were remained within the splats. These precipitates are rich in Al, as detected by the EDS analysis, and are present in the as-received powder as well (see the inset in Fig. 1b).

The characteristics of the coating obtained from depositing the spray-dried WM powder are depicted in Fig. 8. It is clear that a surface with less roughness level compared to the CN coating has been formed. Moreover, the cross-section images exhibit a considerable number of dark veins between the splats, known as the oxide stringers. This has to do with the excessive heating of the small powder particles, resulting in significant in-flight oxidation. Further, the small splat sizes may imply the scattering of the spray-dried powder particles within the HVOF jet stream. More precisely, the high-velocity of the jet stream causes a drop in the pressure, which in turn, can lead to the scattering of porous powder particles [39].

Fig. 9 shows the characteristics of the coating attained from spraying the DM powder. Similar lamellar structure was formed due to the spreading of splats; however, slightly higher content of inter-particle pores was notable for the DM coating. This is mainly due to the insufficient localized particle deformation. The lower deformability of the DM powder particles originates from their high work-hardening level during the milling process. As can be seen from the coating surface, presence of the un-deformed particles leads to the formation of pin-holes. It should be mentioned that these pores are not inter-connected; therefore, they would not exacerbate the penetration of corrosive elements through the coating [40].

When looked at in detail, a sporadic distribution of dark dots was observed for the DM coating (Fig. 10). According to the EDS elemental mapping analysis, these dots are rich in Al and O. Aside from the dark veins in the splat boundary regions, it appears that the dispersed dots stem from the alumina formation and dispersion during the milling process. It should be noted that based on the EDS analysis, it was revealed that the DM powder exhibited higher oxygen content (Fig. 6c). Although the milling process was conducted in a high-purity Ar ambient, the slight powder oxidation occurred due to the temperature rise during milling. The generated temperature is dependent on the energy input into the powder, which can be up to 30 kJ/mol [41]. It has been reported that the addition of fine-grained alumina particles strengthens the high-tem-

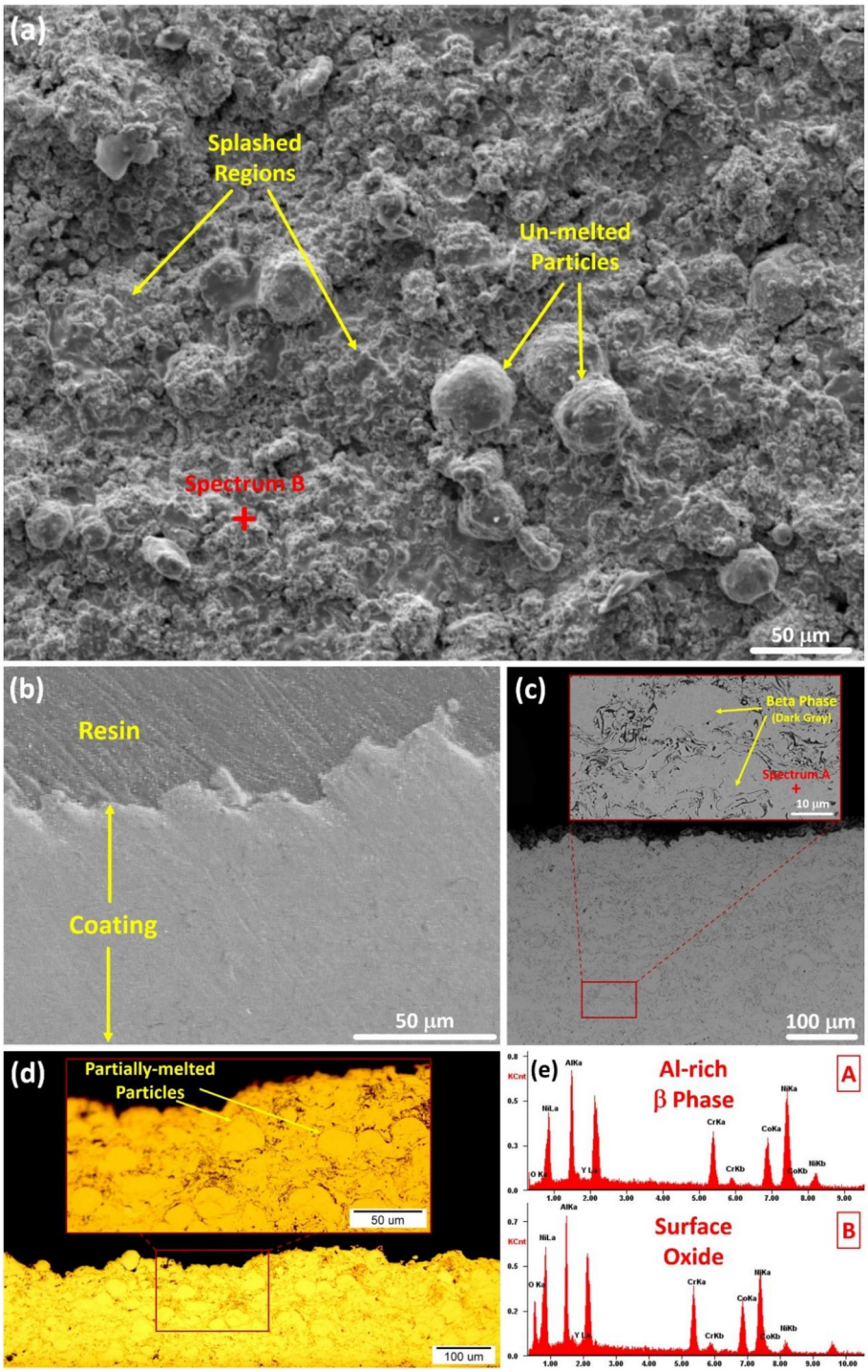

Fig. 7. Characteristics of the CN coating; (a) surface SE-SEM image, (b) cross-section SE-SEM image, (c) cross-section BSE-SEM image, (d) cross-section OM image, and (e) EDS analysis performed on the marked spots.

perature wear and oxidation resistance of the MCrAlY coatings [4, 42].

The Vickers hardness results of the coatings with a typical OM image showing indents from hardness measurements are shown in Fig. 11. As is apparent from Fig. 11b, the measured hardness values vary across the cross-section of the coating. This is due to the discrepancies in the resistance of different regions to the indenter force and the standard deviations in the measurements were indicated by the error bars. Both of the coatings obtained from the milled powders, exhibited higher hardness values compared to the CN coating. The DM coating owns the highest hardness of 519±21 HV_{300}. This is attributable to the combined effect of the presence of work-hardened powder particles and alumina dispersoids within the coating. Furthermore, as discussed earlier, the near-surface regions of the coating lack the hammering effect from the subsequent deposition pass; thus, exhibit slightly lower hardness values (note the large indent size shown in Fig. 11b).

4. Conclusions

The main objective of the work presented in this paper concerned the development of nanocrystalline NiCoCrAlY coatings. In this regard, mechanical milling approach was taken to produce nano-scaled NiCoCrAlY feedstock powder, and then the coatings were applied by means of HVOF spraying method. The key findings are as follows:

1. The wet milling process resulted in the small-sized flaky particles, which required an additional agglomeration step to be used as a sprayable powder. With this in mind, a spray dry-

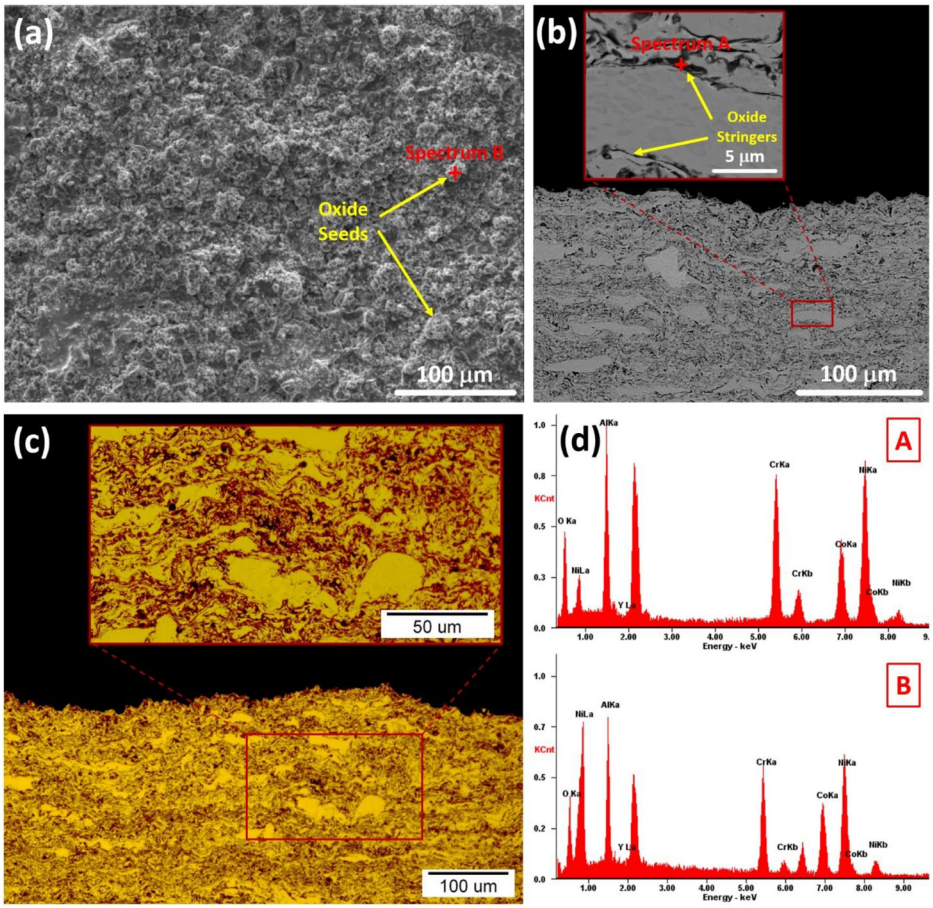

Fig. 8. Characteristics of the WM coating; (a) surface SE-SEM image, (b) cross-section BSE-SEM image, (c) cross-section OM image, and (d) EDS analysis performed on the marked spots.

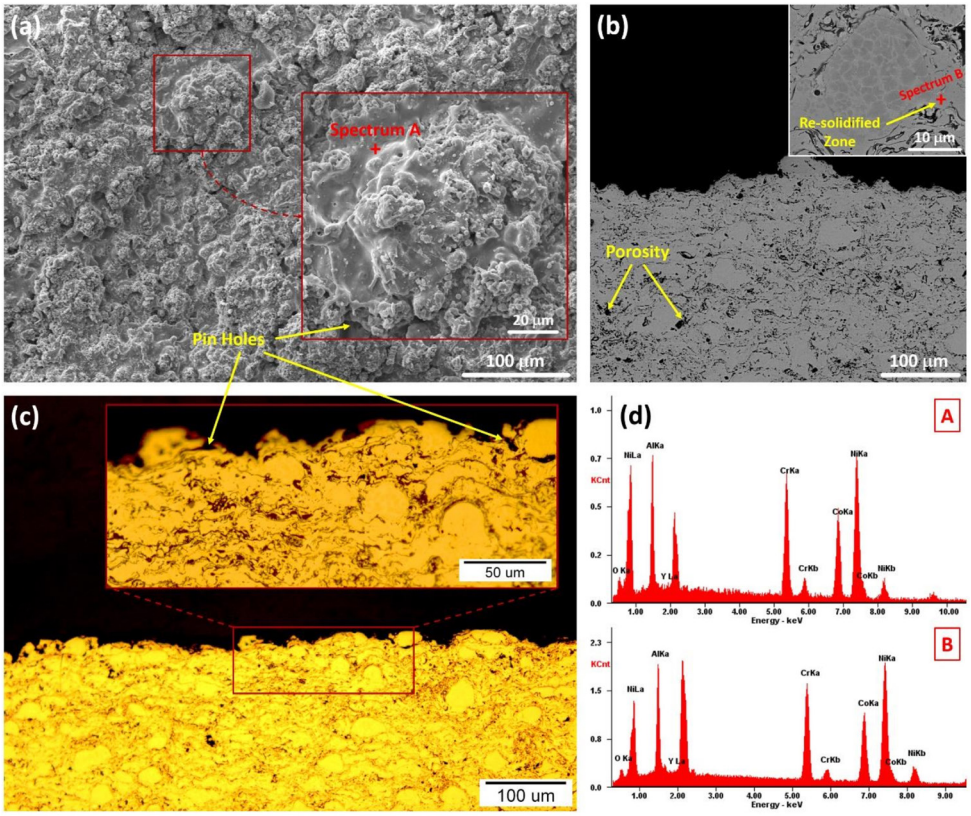

Fig. 9. Characteristics of the DM coating; (a) surface SE-SEM image, (b) cross-section BSE-SEM image, (c) cross-section OM image, and (d) EDS analysis performed on the marked spots.

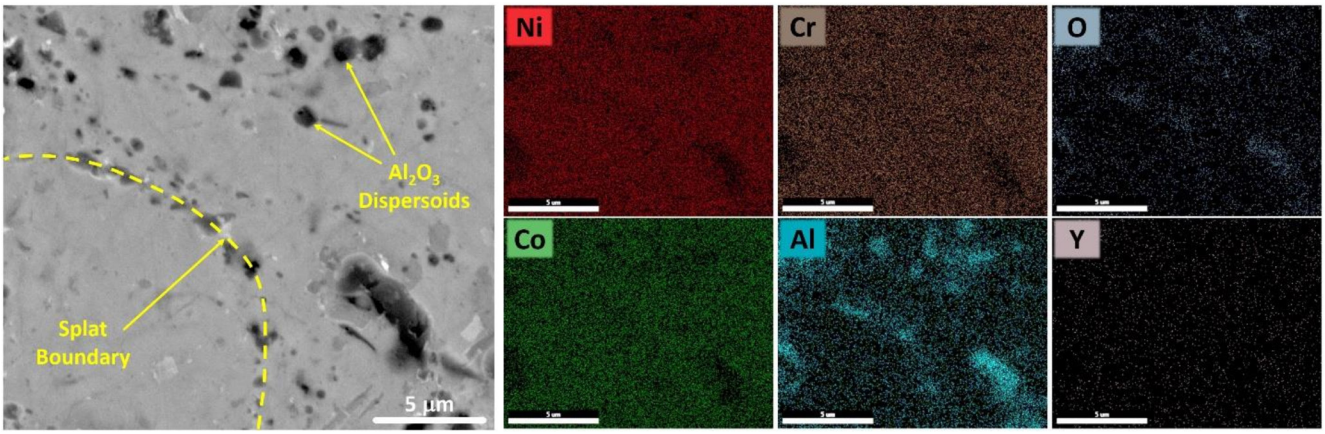

Fig. 10. BSE-SEM image and corresponding EDS elemental mapping from DM coating.

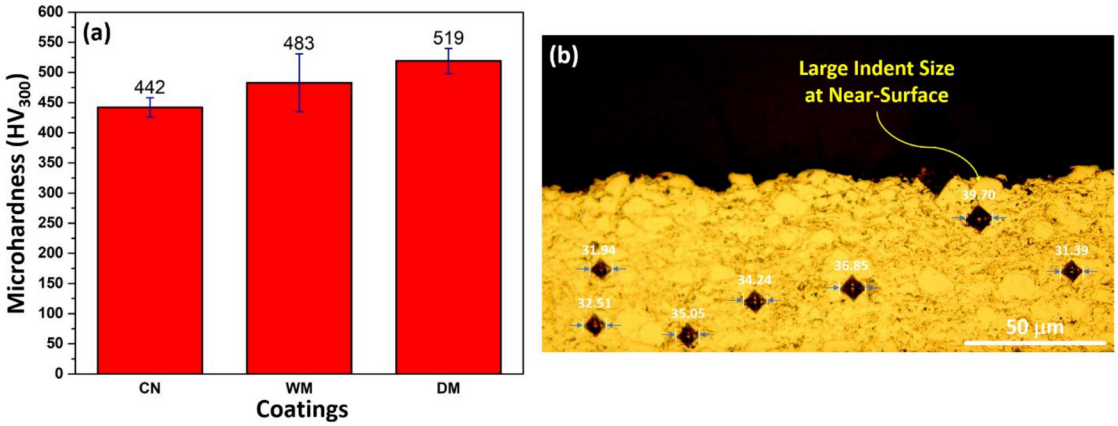

Fig. 11. (a) Average values of hardness measurements and (b) OM image showing indents from hardness measurements for the DM coating.

ing process was conducted, by which porous particles with semi-spherical morphology were achieved.

2. The powder particles obtained by dry milling process were compact with semi-spherical morphology, which met the suitable properties for thermal spraying. It appeared that the dry medium gave rise to a higher energy input into the powder.
3. A slightly higher contamination level was observed for the dry milled powder and it was attributed to the higher wear rates associated in this condition.
4. The coatings' investigations exhibited some discrepancies in terms of porosity and oxide content. These differences were mainly ascribed to the deformability and in-flight oxidation of the powder particles.
5. The coating obtained from spraying the dry milled powder (DM) showed the highest hardness values. This is due to the combined effect of powder particle work-hardening during the milling process and the presence of alumina dispersion within the coating.

Acknowledgments

The authors would like to acknowledge the Tarbiat Modares University for the financial support towards this research.

Conflict of interest

The authors declare that there is no conflict of interest.

REFERENCES

[1] N.P. Padture, M. Gell, E.H. Jordan, Thermal barrier coatings for gas-turbine engine applications, Science 296(5566) (2002) 280-284.

[2] R.C. Reed, The superalloys: fundamentals and applications, Cambridge university press, England, 2008.

[3] F. Ghadami, A. Zakeri, A.S.R. Aghdam, R. Tahmasebi, Structural characteristics and high-temperature oxidation behavior of HVOF sprayed nano-CeO_2 reinforced NiCoCrAlY nanocomposite coatings, Surface and Coatings Technology 373 (2019) 7–16.

[4] F. Ghadami, A. Sabour Rouh Aghdam, A. Zakeri, B. Saeedi, P. Tahvili, Synergistic effect of CeO_2 and Al_2O_3 nanoparticle dispersion on the oxidation behavior of MCrAlY coatings deposited by HVOF, Ceramics International 46(4) (2020) 4556–4567.

[5] M. Bai, H. Jiang, Y. Chen, Y. Chen, C. Grovenor, X. Zhao, P. Xiao, Migration of sulphur in thermal barrier coatings during heat treatment, Materials and Design 97 (2016) 364–371.

[6] M. Bai, Fabrication and Characterization of Thermal Barrier Coatings, PhD thesis, Coventry University, 2015.

[7] T.M. Pollock, S. Tin, Nickel-based superalloys for advanced turbine engines: Chemistry, microstructure, and properties, Journal of propulsion and power 22(2) (2006) 361–374.

[8] W. Xia, X. Zhao, L. Yue, Z. Zhang, Microstructural evolution and creep mechanisms in Ni-based single crystal superalloys: A review, Journal of Alloys and Compounds 819 (2020) 152954.

[9] M. Masoumi Balashadehi, P. Nourpour, A. Sabour Rouh Aghdam, M.H. Allahyarzadeh, A. Heydarzadeh, M. Hamdi, The formation, microstructure and hot corrosion behaviour of slurry aluminide coating modified by Ni/Ni-Co electrodeposited layer on Ni-base superalloy, Surface and Coatings Technology 402 (2020) 126283.

[10] A. Zakeri, E. Bahmani, A. Sabour Rouh Aghdam, B. Saeedi, M. Bai, A study on the effect of nano-CeO
2 dispersion on the characteristics of thermally-grown oxide (TGO) formed on NiCoCrAlY powders and coatings during isothermal oxidation, Journal of Alloys and Compounds 835 (2020) 155319.

[11] B. Song, M. Bai, K.T. Voisey, T. Hussain, Role of Oxides and Porosity on High-Temperature Oxidation of Liquid-Fueled HVOF Thermal-Sprayed Ni50Cr

Coatings, Journal of Thermal Spray Technology 26 (2017) 554–568.
[12] C. Liu, Y. Chen, L. Qiu, H. Liu, M. Bai, P. Xiao, The al-enriched γ'-Ni3Albase bond coat for thermal barrier coating applications, Corrosion Science 167 (2020) 108523.
[13] A. Zakeri, E. Bahmani, A. Sabour Rouh Aghdam, B. Saeedi, A comparative study on the microstructure evolution of conventional and nanostructured MCrAlY powders at high-temperature, Surface and Coatings Technology 389 (2020) 125629.
[14] A. Zakeri, F. Ghadami, A. Sabour Rouhaghdam, B. Saeedi, Study on production of modified MCrAlY powder with nano oxide dispersoids as HVOF thermal spray feedstock using mechanical milling, Materials Research Express 7 (2019) 015030.
[15] W. Brandl, D. Toma, H.J. Grabke, The characteristics of alumina scales formed on HVOF-sprayed MCrAlY coatings, Surface and Coatings Technology 108–109 (1998) 10–15.
[16] B. Saeedi, A. Sabour Rouh Aghdam, G. Gholami, A study on nanostructured in-situ oxide dispersed NiAl coating and its high temperature oxidation behavior, Surface and Coatings Technology 276 (2015) 704–713.
[17] A.H. Pakseresht, Production, properties, and applications of high temperature coatings, SCOPUS, USA, 2018.
[18] A.H. Pakseresht, A. Kimiayi, M. Alizadeh, H. Nuranian, A. Faeghinia, Microstructural study and hot corrosion behavior of bimodal thermal barrier coatings under laser heat treatment, Ceramics International 46(11, Part B) (2020) 19217–19227.
[19] A.C. Karaoglanli, K.M. Doleker, B. Demirel, A. Turk, R. Varol, Effect of shot peening on the oxidation behavior of thermal barrier coatings, Applied Surface Science 354 Part B (2015) 314–322.
[20] Q. Zhang, C.J. Li, C.X. Li, G.J. Yang, S.C. Lui, Study of oxidation behavior of nanostructured NiCrAlY bond coatings deposited by cold spraying, Surface and Coatings Technology 202(14) (2008) 3378–3384.
[21] K.M. Doleker, A.C. Karaoglanli, Comparison of Oxidation Behavior of Shot-Peened Plasma Spray Coatings with Cold Gas Dynamic Spray Coatings, Oxidation of Metals 88(1) (2017) 121–132.
[22] C. Suryanarayana, Mechanical alloying and milling, Progress in materials science 46(1-2) (2001) 1–184.
[23] M. Tahari, M. Shamanian, M. Salehi, Microstructural and morphological evaluation of MCrAlY/YSZ composite produced by mechanical alloying method, Journal of alloys and compounds 525 (2012) 44–52.
[24] L. Ajdelsztajn, J.A. Picas, G.E. Kim, F.L. Bastian, J. Schoenung, V. Provenzano, Oxidation behavior of HVOF sprayed nanocrystalline NiCrAlY powder, Materials Science and Engineering: A 338(1-2) (2002) 33–43.
[25] J.A. Picas, A. Forn, L. Ajdelsztajn, J. Schoenung, Nanocrystalline NiCrAlY powder synthesis by mechanical cryomilling, Powder technology 148(1) (2004) 20–23.
[26] L. Ajdelsztajn, F. Tang, G.E. Kim, V. Provenzano, J.M. Schoenung, Synthesis and oxidation behavior of nanocrystalline MCrAlY bond coatings, Journal of Thermal Spray Technology 14(1) (2005) 23–30.
[27] O. Maranho, D. Rodrigues, M. Boccalini, A. Sinatora, Influence of parameters of the HVOF thermal spray process on the properties of multicomponent white cast iron coatings, Surface and Coatings Technology 202(15) (2008) 3494–3500.
[28] ASTM E384-05a, Standard Test Method for Microindentation Hardness of Materials, ASTM Int. 14 (2005) 1–24.
[29] A. Zakeri, E. Bahmani, A.S.R. Aghdam, Impact of MCrAlY feedstock powder modification by high-energy ball milling on the microstructure and high-temperature oxidation performance of HVOF-sprayed coatings, Surface and Coatings Technology 395 (2020) 125935.
[30] D. Guo, L. Zhao, B. Jodoin, Cold Spray for Production of In-Situ Nanocrystalline MCrAlY Coatings – Part II: Isothermal Oxidation Performance, Surface and Coatings Technology 409 (2021) 126828.
[31] Y. Chen, X. Zhao, P. Xiao, Effect of microstructure on early oxidation of MCrAlY coatings, Acta Materialia 159 (2018) 150–162.
[32] S. Hong, Y. Wu, G. Li, B. Wang, W. Gao, G. Ying, Microstructural characteristics of high-velocity oxygen-fuel (HVOF) sprayed nickel-based alloy coating, Journal of Alloys and Compounds 581 (2013) 398–403.
[33] Z. Khodsiani, H. Mansuri, T. Mirian, The effect of cryomilling on the morphology and particle size distribution of the NiCoCrAlYSi powders with and without nano-sized alumina, Powder technology 245 (2013) 7–12.
[34] M.R. Loghman-Estarki, M. Pourbafrany, R. Shoja Razavi, H. Edris, S.R. Bakhshi, M. Erfanmanesh, H. Jamali, S.N. Hosseini, M. Hajizadeh-Oghaz, Preparation of nanostructured YSZ granules by the spray drying method, Ceramics International 40(2) (2014) 3721–3729.
[35] K. Ma, F. Tang, J.M. Schoenung, Investigation into the effects of Fe additions on the equilibrium phase compositions, phase fractions and phase stabilities in the Ni-Cr-Al system, Acta Materialia 58(5) (2010) 1518–1529.
[36] M. Bai, B. Song, L. Reddy, T. Hussain, Preparation of MCrAlY–Al_2O_3 Composite Coatings with Enhanced Oxidation Resistance through a Novel Powder Manufacturing Process, Journal of Thermal Spray Technology 28 (2019) 433–443.
[37] B. Rajasekaran, G. Mauer, R. Vaßen, Enhanced characteristics of HVOF sprayed MCrAlY bond coats for TBC applications, Journal of thermal spray technology 20 (2011) 1209–1216.
[38] S. Deshpande, S. Sampath, H. Zhang, Mechanisms of oxidation and its role in microstructural evolution of metallic thermal spray coatings - Case study for Ni-Al, Surface and Coatings Technology 200(18-19) (2006) 5395–5406.
[39] H. Wang, Y. Liu, X. Ning, Q. Wang, F. Wang, D. Chen, The influence of milling parameters on the characteristics of milled and spray-dried NiCoCrAlY–Al2O3 composite powders, Powder Metallurgy 60(1) (2017) 15–21.
[40] P. Richer, M. Yandouzi, L. Beauvais, B. Jodoin, Oxidation behaviour of CoNiCrAlY bond coats produced by plasma, HVOF and cold gas dynamic spraying, Surface and Coatings Technology 204(24) (2010) 3962–3974.
[41] C. Borchers, T. Stoltenhoff, M. Hahn, M. Schulze, H. Assadi, C. Suryanarayana, F. Gärtner, T. Klassen, Strain-induced phase transformation of MCrAlY, Advanced Engineering Materials 17(5) (2015) 723–731.
[42] H.Y. Wang, D.W. Zuo, M. Di Wang, G.F. Sun, H. Miao, Y.L. Sun, High temperature frictional wear behaviors of nano-particle reinforced NiCoCrAlY cladded coatings, Transactions of Nonferrous Metals Society of China 21(6) (2011) 1322–1328.